

MORPHOLOGIC ANALYSES BY SUMMIT LEVEL AND BASE LEVEL MAPS BASED ON THE ASTER GDEM FOR MORRO DE SÃO JOÃO FELSIC ALKALINE MASSIF, STATE OF RIO DE JANEIRO, BRAZIL

Akihisa MOTOKI ¹, Samuel da SILVA ², Susanna Eleonora SICHEL ², Kenji Freire MOTOKI ³

(1) Departamento de Mineralogia e Petrologia Ígnea, Universidade do Estado do Rio de Janeiro (DMPI/UERJ). Rua São Francisco Xavier 524, Sala A-4023, Maracanã, Rio de Janeiro, CEP 20550-900, RJ. Endereço eletrônico: motokiakihisa@gmail.com.

(2) Departamento de Geologia, Universidade Federal Fluminense (LAGEMAR/UFF). Av. General Milton Tavares de Souza s/n, 4º andar, Gragoatá, Niterói, CEP. 24210-340, RJ. Endereço eletrônico: susannasichel@id.uff.br; samueltec@gmail.com; kenji_dl@hotmail.com.

Introduction
Highlighted methodologies
Regional geology
Morro de São João intrusive body
Summit level maps
Base level maps
Macro concavity index (MCI)
Drainage system
Landform origin
Conclusion
Acknowledgement
Reference

RESUMO - Motoki, A. Silva, S., Sichel, S.E., Motoki, K.F. *Análises geomorfológicas pelos mapas de seppômen e sekkokumen baseado no GDEM de ASTER para o maciço intrusivo de rochas alcalinas félsicas de Morro de São João, RJ.* Este trabalho apresenta as análises morfológicas para o maciço de rochas alcalinas félsicas do Morro de São João, RJ, com o auxílio das técnicas de seppômen e sekkokumen e o modelo digital de elevação de satélite ASTER (GDEM). Os mapas de seppômen mostram a escarpa marginal íngreme de cerca de 30°, o platô virtual de 480 m a 500 m de altitude e a saliência de topo com altura relativa de 150 m. A escarpa marginal tem alta declividade não somente nos mapas de seppômen como também de sekkokumen. Os mapas para a diferença entre o seppômen e sekkokumen, denominados mapas de kifukuryô, demonstram a zona de alta declividade ao longo da borda do corpo e relevos suaves no planalto central. Essas observações indicam alta resistência erosiva das rochas constituintes deste maciço. As drenagens apresentam um sistema radial. Essas são rasas, curtas e íngremes, em média, 20 m de profundidade, 1.1 km de comprimento e 22° de declividade. A maioria das drenagens tem perfil longitudinal quase linear, e não, côncavo. O índice de macro concavidade (MCI) é -1.2, indicando que a forma tridimensional geral deste maciço é altamente convexa, que é muito diferente daquele de edifícios vulcânicos. A morfologia cônica deste maciço não é originada de um vulcão extinto, mas erosão diferencial da intrusão de nefelina sienito, que tem forte resistência à erosão devido à firmeza mecânica e passividade intempérica.

Palavras-chave: seppômen, sekkokumen, GDEM, ASTER, Morro de São João, passividade intempérica.

ABSTRACT - This paper presents morphological analyses for Morro de São João felsic alkaline intrusive massif, State of Rio de Janeiro, Brazil, with the help of summit level and base level map techniques and the satellite digital elevation model of ASTER (GDEM). The summit level maps shows the steep marginal scarp of about 30°, the virtual plateau of 480 m to 500 m of altitude, and the top swell with relative height of 150 m. The marginal scarp is steep, not only on the summit level maps but also on the base level ones. The maps for the difference between summit and base levels, called relief amount map, demonstrate the presence of high declivity zone along the border of the intrusive body and gentle relief area on the central highland. These observations indicate high erosive resistance of the constituent rocks of this massif. The drainages form a radial system. They are shallow, short, and steep, in average 20 m deep, 1.1 km long, and of 22° in declivity. Most of the longitudinal profiles are straight and not concave. The macro concavity index (MCI) is -1.2, showing that the general 3D form of this massif is highly convex, which is widely different from that of volcanic edifices. Therefore, the conical form of this massif is not originated from an extinct volcano, but differential erosion of the nepheline syenite intrusion, which has strong erosive resistance due to mechanical firmness and weathering passivity.

Keyword: summit level map, base level map, GDEM, ASTER, Morro de São João, weathering passivity.

INTRODUCTION

The Morro de São João massif is situated at S22°32.4', W42°01.7', between Casimiro de Abreu, Rio das Ostras, and Barra

de São João, in the central part of the State of Rio de Janeiro, at about 128 km to east-northeast of the city of Rio de Janeiro, Brazil

(Figure 1). This massif is about 650 m of relative height standing up on the near sea-level alluvial plane.

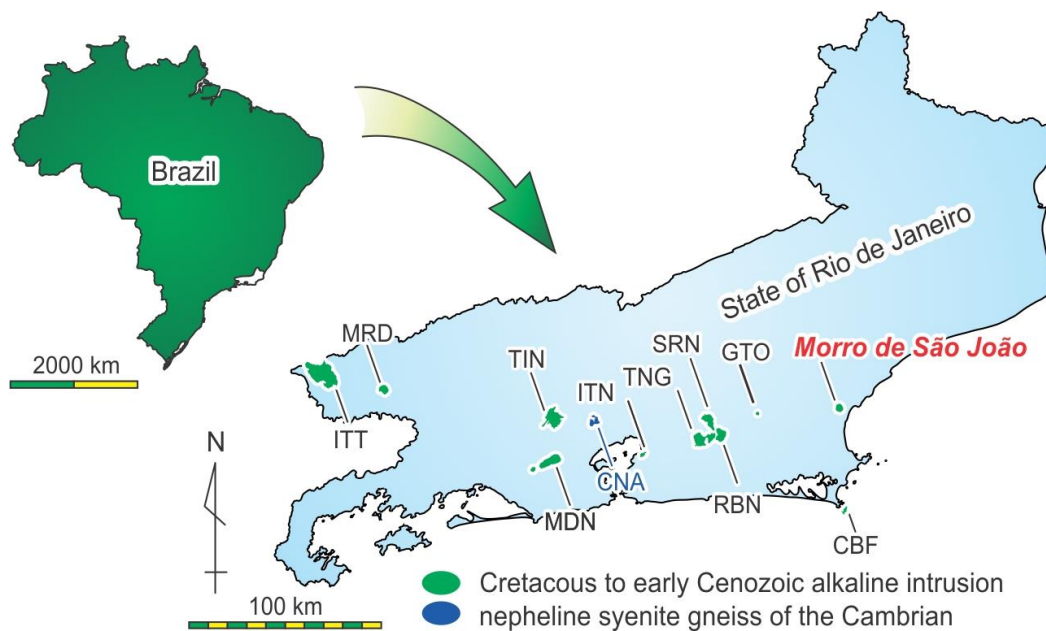


Figure 1. Locality of Morro de São João felsic alkaline intrusive massif in Poços de Caldas - Cabo Frio magmatic alignment, modified from Motoki et al. (2011). ITT - Itatiaia; MRD - Morro Redondo; TNG - Tinguá; ITN - Itáúna; TNG - Tanguá; SRN - Soarinho; RBN - Rio Bonito; GTO - Morro dos Gatos; MSJ - Morro de São João; CBF - Cabo Frio Island.

The previous geologic studies demonstrated that it is constituted mainly by early Cenozoic nepheline syenite (Brotzu et al., 2007; Mota et al., 2009), which is incompatible with the popular idea of extinct volcano. Up to the present no detailed geomorphological studies have been performed in order to examine the peculiar landform origin.

The authors have accomplished morphologic analyses of this massif using summit level and base level techniques based on the satellite-derived DEM of ASTER, called ASTER GDEM. The present article shows the results and considers its landform origin.

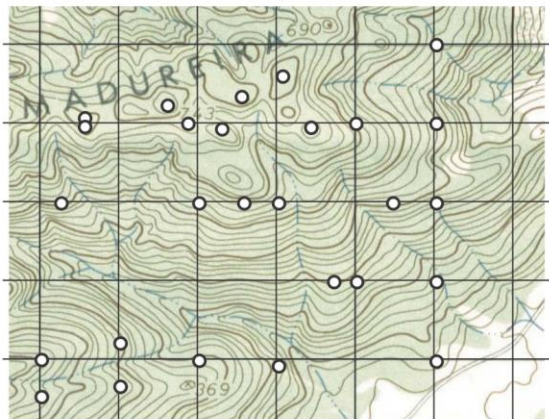
HIGHLIGHTED RESEARCH METHODS

Summit level map (*seppômen*) is a virtual topographic map that reconstitutes virtually the palaeo-geomorphology before vertical erosion by drainages. Base level map (*sekkokumen*) is a virtual topographic map that predicts the future morphology that will be formed by development of lateral erosion of the present drainages. The relief amount (*kifukuryo*) is the difference between summit level and base level surface. These virtual maps are useful for geomorphological studies of volcanic edifices (e.g. Vilaro et al., 1996; Malengreau et al., 1999; Rust et al., 2005; Okuma et al., 2009), vertical tectonic movements (e.g. Deffontaines

et al., 1994; Riis, 1996; Martin, 1966; Huzita & Kasama, 1977; Ferhat et al., 1998; Kühni & Pfiffener, 2001; Sato & Raim, 2004; Motoki et al., 2009a), and erosive resistance of massifs (e.g. Motoki et al., 2008a; Silva 2010).

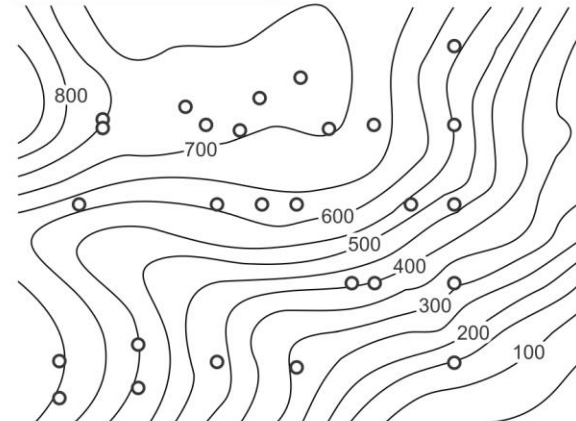
Summit level map is constructed by the following steps (Figure 2): 1) Divide the original topographical map in small squares by a grid of defined interval; 2) Mark the highest point of each square area; 3) Make a new topographical map only by the marked points. Base level map is constructed by similar procedures but based on the lowest point of each square.

A. Original topographic map



○ highest point

B. Summit level map



C. Grid interval effect

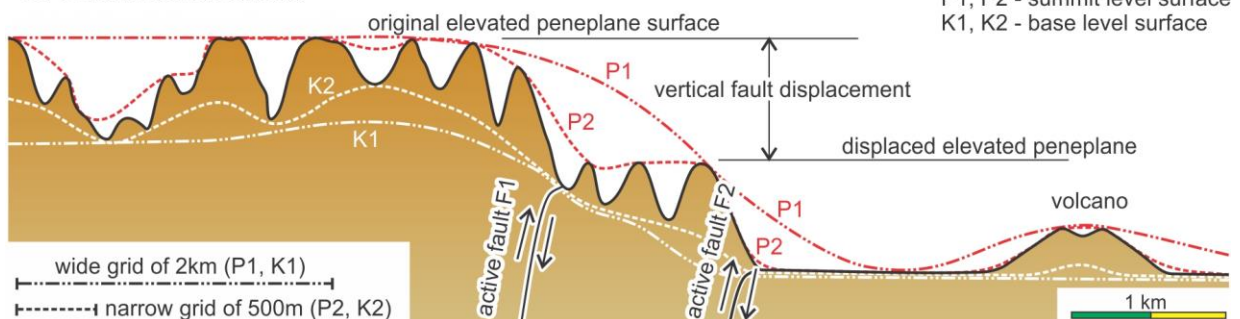


Figure 2. Confection procedures of summit level map (A, B) and of grid interval effects for summit level and base level maps (C), modified from Motoki et al. (2008a).

The authors adopt satellite-derived digital elevation model for the base topographic data. ASTER (Advanced Spaceborne Thermal Emission and Reflection) is thermal remote sensing component installed on satellite TERRA. From 2009, ERSDAC (Earth Remote Sensing Analyses Center) released the satellite DEM elaborated by radar altimetry, called GDEM (Global Digital Elevation Map). GDEM covers all of the areas of the world between 60°N and 60°S. Its horizontal resolution is 1 second, which corresponds to 30 m in equatorial region, which is three times better than SRTM (Shuttle Rader Topographic Model). In spite of few small problems, GDEM

is evaluated as of high reliability (Hirt et al., 2010; Chrysoulakis et al., 2011). The data can be downloaded from the homepage of ERSDAC:

<http://www.gdem.aster.ersdac.or.jp/index.jsp>.

The original data of GDEM, of GeoTiff format, are converted to ASCII format by GIS software, such as ArcGis™, Spring™, and GMT™. The summit level and base level maps are generated by the original software BAZ ver. 1.0 built 71, which elaborates simultaneously summit level, base level, and relief amount maps of the grid intervals of 1920 m, 960 m, 480 m, 120 m, and 60 m (Figure 3).

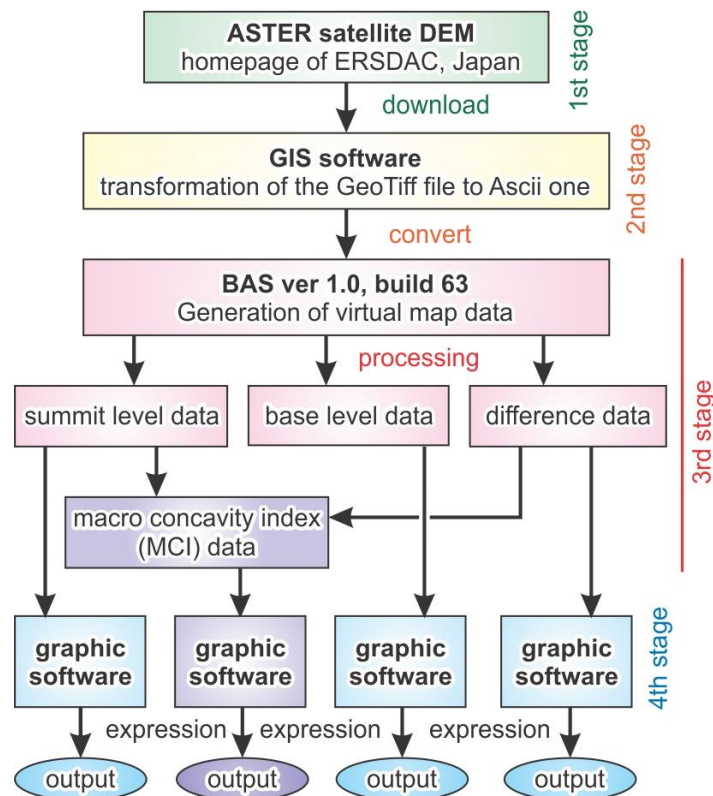


Figure 3. Working flowchart of BAZ system, ver. 1.0, built 71.

The grid interval is an important factor. The summit level map of a narrow grid interval presents palaeo-geomorphology of a near past with detailed features, and the virtual map based on a wide interval shows palaeo-geomorphology of a remote past in ambiguous way (Figure 2C). Similar tendencies are present in base level and relief amount maps.

For the morphologic analysis of felsic alkaline massifs of the State of Rio de Janeiro, such as Morro de São João, the grid interval of 0.5 km to 1 km is convenient. For an elevated peneplane, that of 2 km to 4 km is recommended (Aires et al., 2012). Comparative observation of the virtual maps of different grid intervals enables the reconstitution of water system evolution history.

REGIONAL GEOLOGY

The region is underlain mainly by leucocratic granitic orthogneiss of the Regiões de Lagos Unit and partially by mafic gneiss of the São Mateus (Schmitt et al., 2004). They constitute Cabo Frio Terrane, which is South American extension of the Congo Craton (Heilbron et al., 2000; Heilbron & Machado, 2003). The intrusion age of the granite is about 1950 Ma, corresponding to the Trans-Hudsonian or the Trans-Amazonian orogeny. The metamorphic age is about 530 Ma, which is of the Pan-African or the Ribeira continental collision event (Schmitt et al., 2004; Motoki & Orihashi, unpublished data). They were cut by silicified tectonic breccia of the late stage of Pan-African orogeny (Motoki et al., 2011;

2012a). This basement was cut by early Cretaceous mafic dykes that correspond to a part of feeders of the continental flood basalt of Paraná Province (Stewart et al., 1996; Guedes et al., 2005; Motoki et al., 2009b).

All of them were intruded by late Cretaceous to Early Cenozoic felsic alkaline bodies (Sichel et al., 2012; Figure 4), such as: Itatiaia (Brotzu et al., 1997), Morro Redondo (Brotzu et al., 1989), Tinguá (Derby, 1897), Mendanha (Motoki et al., 2007a; Petrakis et al., 2009), Itaúna (Motoki et al., 2008b), Tanguá, Rio Bonito, Soarinho (Motoki et al., 2010), Morro dos Gatos (Motoki et al., 2012b), and Cabo Frio Island (Sichel et al., 2008; Motoki & Sichel, 2008; Motoki et al., 2008c). They form

the Poços de Caldas - Cabo Frio alkaline magmatic alignment (Thomáz Filho & Rodrigues, 1999). The Morro de São João

intrusive body (Brotzu et al., 2007; Mota et al., 2009) is the east-most member of this magmatic alignment.

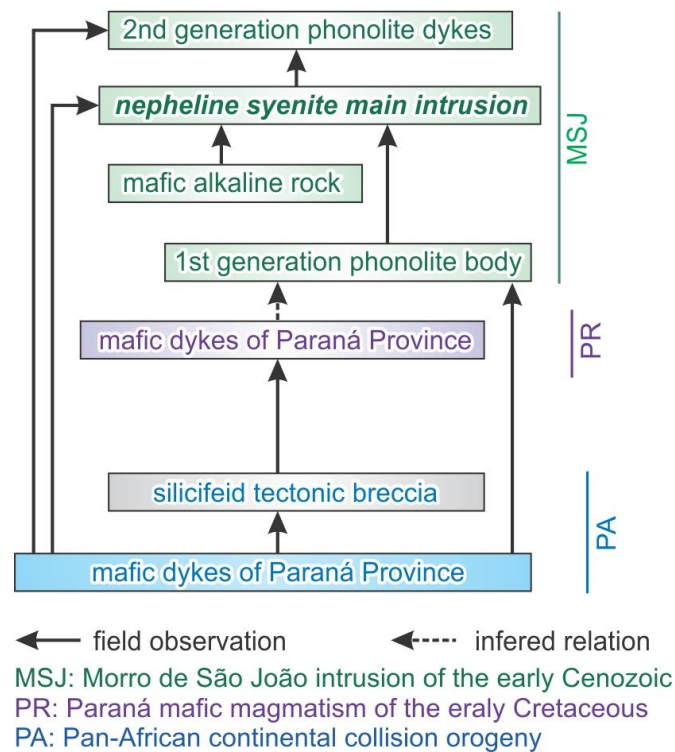


Figure 4. Intrusive relation between the rock bodies of the Morro de São João felsic alkaline intrusion area.

MORRO DE SÃO JOÃO INTRUSIVE BODY

The Morro de São João is a semi-circular massif of 4 km x 4.7 km with relative height of about 650 m, which stands up on the sea level alluvial plane. Almost all of the parts of the massif are composed of the alkaline rocks. According to the pixel counting method by Wilbur ver. 1.0 (Motoki et al., 2006; 2007b), the measured distribution area is 14.4 km².

The ASTER GDEM topographic data indicate that the highest point of the Morro de São João is 673 m above sea level. However, there are some different previous versions, such as: 816 m after a newspaper article of o Globo; 729 m after a sightseeing promotion agency.

The country rock of the felsic alkaline intrusion is orthogneiss, which is exposed at the foot of the massif. The half-orange hills of about 100 m of altitude (Aires et al., 2012), made up of the basement gneiss, are observed

also in this area. The alluvial lowland is covered by Quaternary beach sand deposits, which is about 5 m thick. This material is extracted as high-quality construction material (Petrakis et al., 2009).

Morro de São João massif is constituted mainly by nepheline syenite with local occurrences of pseudoleucite nepheline syenite, phonolite (Photo 1). The rocks are remarkably undersaturated in silica (Brotzu et al., 2007) with high modal content of feldspathoids. The main constituent minerals are alkaline feldspar and nepheline. They are vulnerable to chemical weathering under the tropical climate. The intrusive body has a flattened coffee filter-like general three-dimensional form and the present exposure corresponds to the horizontal section of middle to upper level of the body (Figure 5).



Photo 1. Constituent rocks of the Morro de São João intrusive body, State of Rio de Janeiro, Brazil: **A)** Nepheline syenite of contact zone; **B)** Pseudoleucite nepheline syenite cut by small phonolite dyke; **C)** Mafic alkaline rock captured by nepheline syenite magma; **D)** Nepheline syenite with well-developed fluting fabric on the surface.

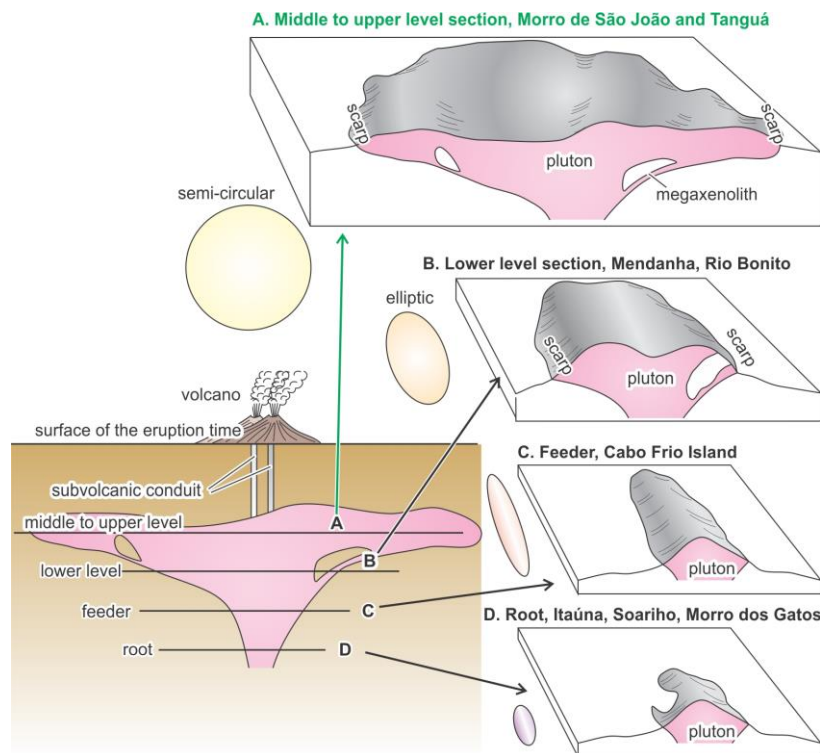


Figure 5. Three-dimensional form of the Cretaceous to early Cenozoic felsic alkaline intrusive bodies of the State of Rio de Janeiro, Brazil, which show horizontal sections of different relative levels, modified from Motoki et al. (2008a): **A)** Middle to upper part with semi-circular body in the geologic map, such as Morro de São João and Tanguá; **B)** Lower section cropping out an elliptic body, Mendanha and Rio Bonito; **C)** Feeder fissure, Cabo Frio Island; **D)** Pluton root, Itaúna, Soarinho, Morro dos Gatos.

SUMMIT LEVEL MAPS

The Figure 6 shows the summit level maps of Morro de São João massif based on grid intervals of 1920 m, 960 m, 480 m, 240 m, 120 m, and 60 m, which have been constructed with the help of the BAZ system based on GDEM.

The map of 1920 m grid interval (Figure 6A) presents conical virtual form the massif. The map of 960 m mesh interval (Figure 6B) similar form but shows high-angle scarps and relatively flat narrow top. The mountain slope is smooth, indicating that there are no morphologic characteristics larger than 1 km.

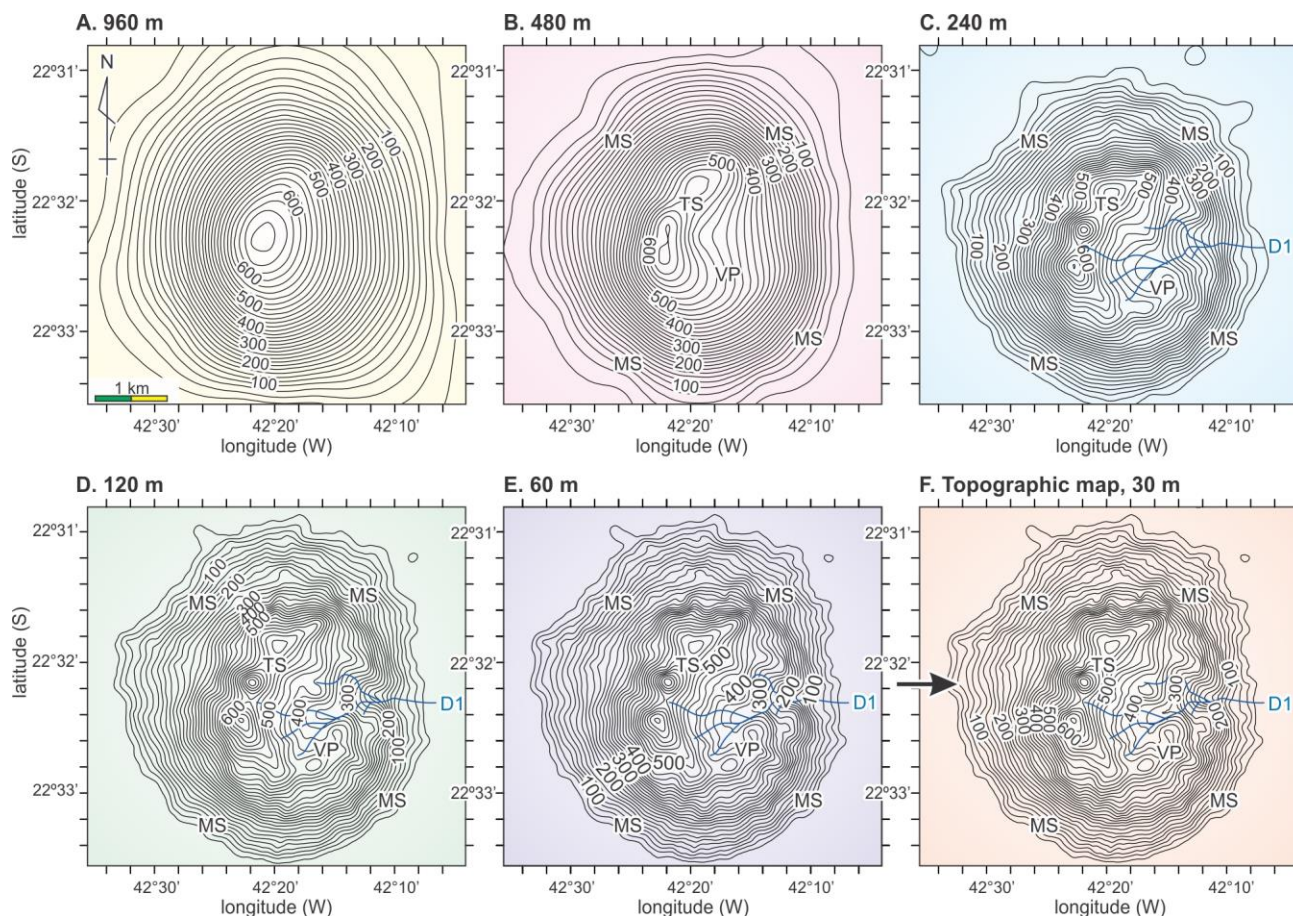


Figure 6. Summit level maps for Morro de São João, State of Rio de Janeiro, Brazil, based on the grid intervals of: **A)** 960 m; **B)** 480 m; **C)** 240 m; **D)** 120 m; **E)** 60 m. The map **F)** shows original GDEM map with the resolution of 30 m. MS - marginal scarp; VP - virtual plateau; TS - top swell; D1 - The largest drainage in the massif.

The summit level map of 480 m grid interval (Figure 6C) shows the marginal scarp (MS), the virtual plateau (VP), and the top swell (TS). The virtual plateau is 480 m to 500 m above sea level and constituted by high crests and a deep valley. Therefore, it does not correspond to a remnant elevated peneplane. The marginal scarp is of high-angle, about 25°, and surrounds the vertical plateau.

The map of 240 m mesh interval (Figure 6D) demonstrates that some parts of the marginal scarp are of very high-angle, with

maximum declivity of 28° on north and north-west slope. The northwest slope, in which mafic alkaline rock xenoliths occur, shows local occurrence of slightly concave form, however no morphology suggestive of landslide deposit is found.

The summit level map of 120 m grid interval (Figure 6D) presents the same characteristics of the massif slope. On this map, the virtual plateau is not relevant because of the erosion of the drainage D1.

In this scale, the summit level maps of narrower mesh intervals (Figure 6E, F) are very similar to the original topographic map of GDEM. Around the border of this massif, no relevant landslide deposit morphology is found with the exception of west-northwest slope (Figure 6F, black arrow).

These summit level maps confirm the existence of the high-angle marginal scarp, the central virtual plateau, and the top swell in the

Morro de São João felsic alkaline intrusive massif. They are characteristic of the massifs originated from differential erosion of the felsic alkaline intrusive bodies of this region (Silva, 2010). The Figure 7 shows horizontal silhouette of the summit level surface of 240 m grid interval and field photo of the same angle. The mountain silhouette represents highest points of the massif, and therefore, the sights of certain angles are similar to those of summit level.

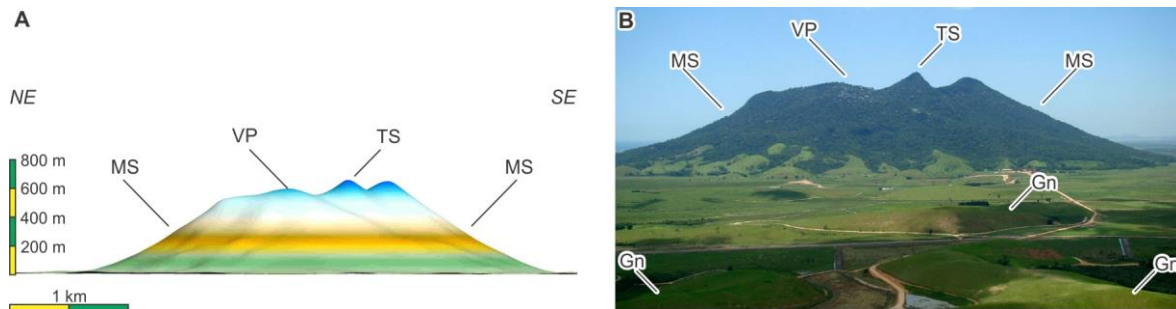


Figure 7. The marginal scarp (MS), the virtual plateau (VP), and the top swell (TS) expressed on the silhouette of summit level surface of the 240 m grid interval (A) and field photograph (B). The photograph is the credit of geologist Wilson Oliveira, presented by Oscar Braun. MS - marginal scarp; VP - virtual plateau; TS - top swell; Gn - half-orange hill of the basement gneiss.

BASE LEVEL MAPS

The Figure 8 shows the base level maps with the mesh intervals of 960 m, 480 m, and 240 m. Those of the 120 m and 60 m grid intervals are not shown because of the similarity to the original topographic map of GDEM.

The map of 960 m grid interval (Figure 8A) shows conical virtual form of the massif

with small flat top area. The map of 480 m mesh interval (Figure 8B) demonstrates virtual plateau (VP) and top swell (TS). The marginal scarp (MS) is clear, steep and high. The elliptic form suggests that the erosion on east and west slopes is more intense than north and south ones.

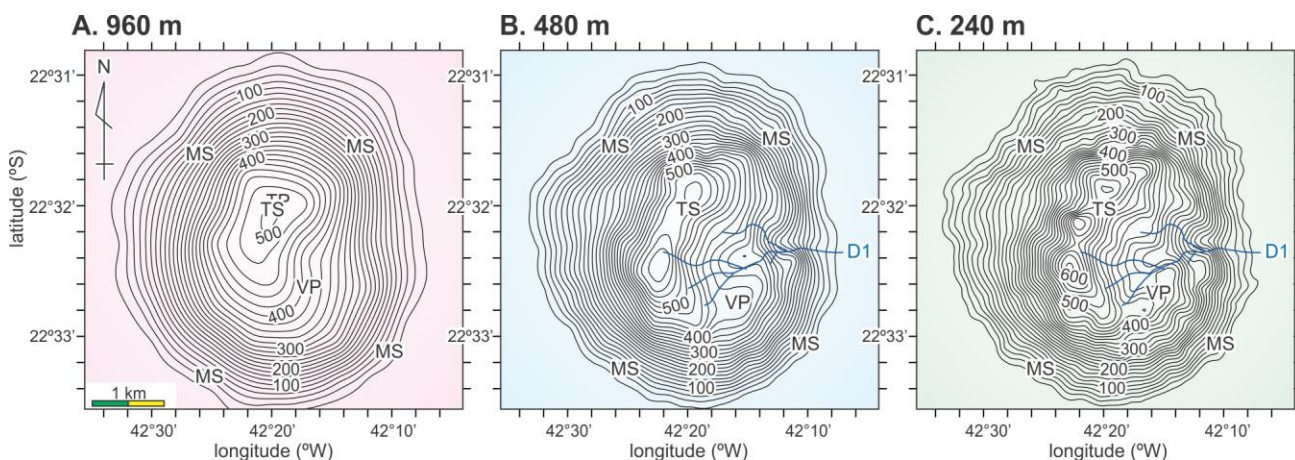


Figure 8. Base level maps for Morro de São João felsic alkaline intrusive massif of the grid intervals of: A) 960 m; B) 480 m; C) 240 m. D1 - the largest drainage of the massif.

The map of 240 m mesh interval (Figure 8C) expresses virtual plateau, top swell, and marginal scarp more expressively. Although the surface is of base level map, the marginal scarp is very steep, up to 30°. The fact indicates that the drainages on the marginal scarp are shallow, and therefore, the constituent rocks have very high erosive resistance.

The Figure 9 presents the maps of the difference height between summit level and

base level surfaces based on grid intervals of 960 m, 480 m, and 240 m called relief amount maps (*kifukuryo*). It is notable that on all of these maps the high declivity zones (blue and white zones) are present along the massif border (MS) and relatively flat zones (yellow and green areas) are present on the highland (VP, TP). The castle wall-like swells on these figures are characteristics of the morphology of the felsic alkaline rock massifs of this region.

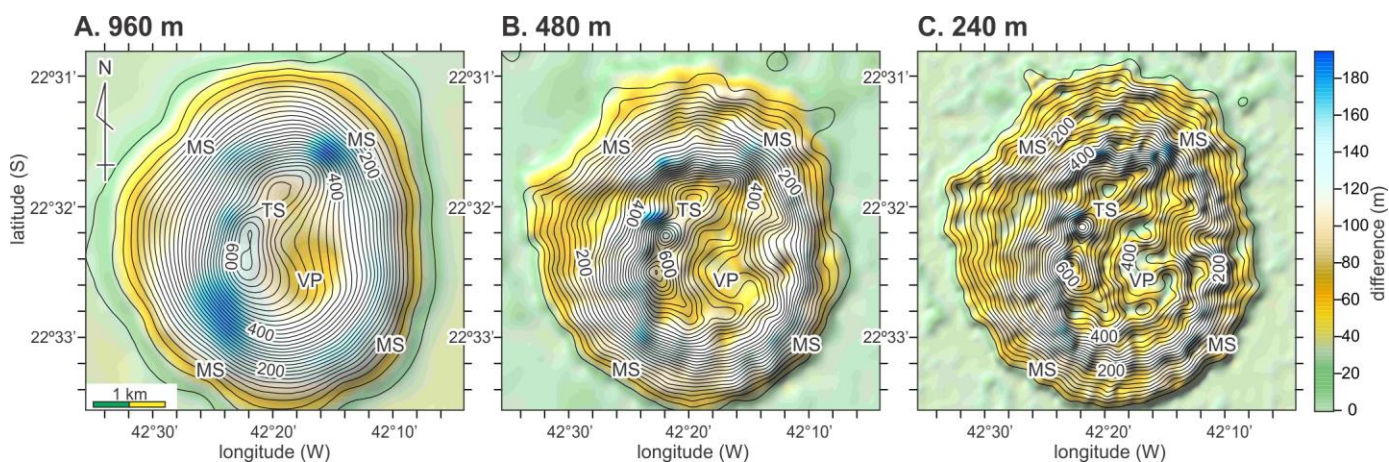


Figure 9. The maps of the difference between the summit level height and the base level one, called relief amount maps (*kifukuryo*) with the grid intervals of: **A)** 960 m; **B)** 480 m; **C)** 240 m.

MACRO CONCAVITY INDEX (MCI)

An intensely eroded massif with highly developed drainages is made up of acute peaks and deep valleys, and therefore, has high declivity. Its general 3D form is concave. On the other hand, a massif with little effects of erosion is composed of shallow and wide drainages and of low declivity, so it has convex general form.

General three-dimensional form of a massif, in relation to convex or concave, can be expressed by the diagram between summit level (horizontal axis) and the difference between summit level and base level height, that is, the relief amount (vertical axis). The “a” constant of the quadric equation ($y=ax^2+bx+c$) of the second order polynomial regression for the projected points on this diagram is the key parameter.

A massif of convex general form has negative “a” constant. On the other hand, a concave massif has “a” constant of positive or close to zero (Motoki et al., 2012c). Therefore, the three-dimensional form of the felsic alkaline

rock massifs originated from differential erosion and the young composite volcano edifices are widely different. These authors proposed 1000 times of the “a” constant as the “macro concavity index” (MCI). This index represents general landform of the whole massif, so it is different from the conventional concavity index for longitudinal profile of drainage (Wells et al., 1988; Kirby & Whipple, 2001; Rãdoane, et al., 2003).

The Figure 10A presents the above-mentioned diagram, called MCI diagram, based on 480 m grid for Morro de São João massif. The Figure 10B shows the comparison between felsic alkaline massifs with convex form and young composite volcanoes with concave form.

The MCI parameter of the Morro de São João is -1.2, being lower than that of Mendanha and Tanguá bodies. That is, its 3D form is highly convex. This phenomenon can be attributed to the absence of notable vertical erosion along fracture system and of hydrothermal zone and the nepheline syenite of

Morro de São João shows directly its erosive resistance.

The highly silica-undersaturated composition of the nepheline syenite could have intensified the weathering passivity effects. That is, the regolith is composed of clay

minerals originated from chemical weathering of nepheline and alkaline feldspar. It is impermeable and protects from the surface water percolation into the rock body (Motoki et al., 2008a).

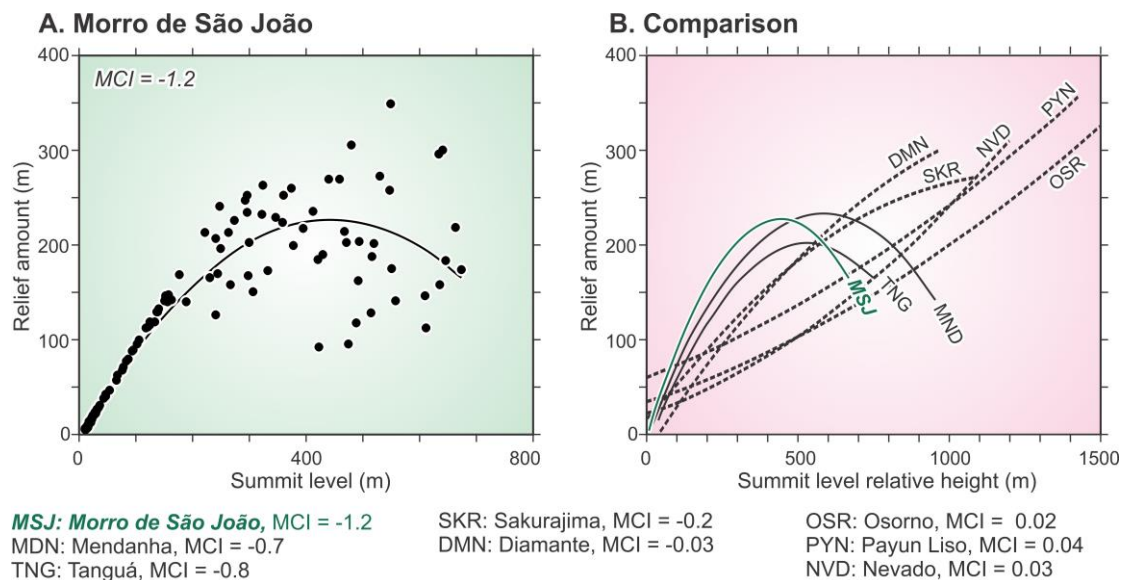


Figure 10. The diagram expressing the relation between summit level and the the relief amount, called MCI diagram, for Morro de São João massif (A). The diagram B shows the comparison between felsic alkaline rock massifs and young composite volcanoes. The grid interval is 480 m. The data with the exception of Morro de São João are originated form Motoki et al., (2012b) and unpublished ones data of the authors. MSJ - Morro de São João massif; MND - Mendanha alkaline massif; TNG - Tanguá massif (felsic alkaline intrusion of the State of Rio de Janeiro, Brazil); SKR - Sakurajima volcano (Kyushu Island, Japan); DMN - Cerro de Diamante volcano, NVD - Nevado volcano; PYN - Payún Liso volcano (Mendoza, Argentina), OSR - Osorno volcano (Chile).

DRAINAGE SYSTEM

In total, 19 drainages more than 300 m long of the Moro de São João massif are observed. They constitute a radial system (Figure 11A) and have little developed branches. The drainages are short, steep, and shallow, in average 1.1 km long, 410 m in relative height, and 22° of declivity (Figure 11B). Only the largest drainage (D1) cuts the centre of the massif which is 180 m deep. The others are in general less than 25 m deep and present on the marginal scarp.

Their longitudinal declivity is very high, with maximum angle of 27°. Most of the drainages have almost straight longitudinal profile with the concavity index next to zero (Figure 11C). The D1 is exceptional and has double stage profile. These characteristics are common in felsic alkaline intrusive massifs of this region (Silva, 2010), such as Mendanha (Motoki et al., 2008a). The drainages of the Morro de São João are the more expressive.

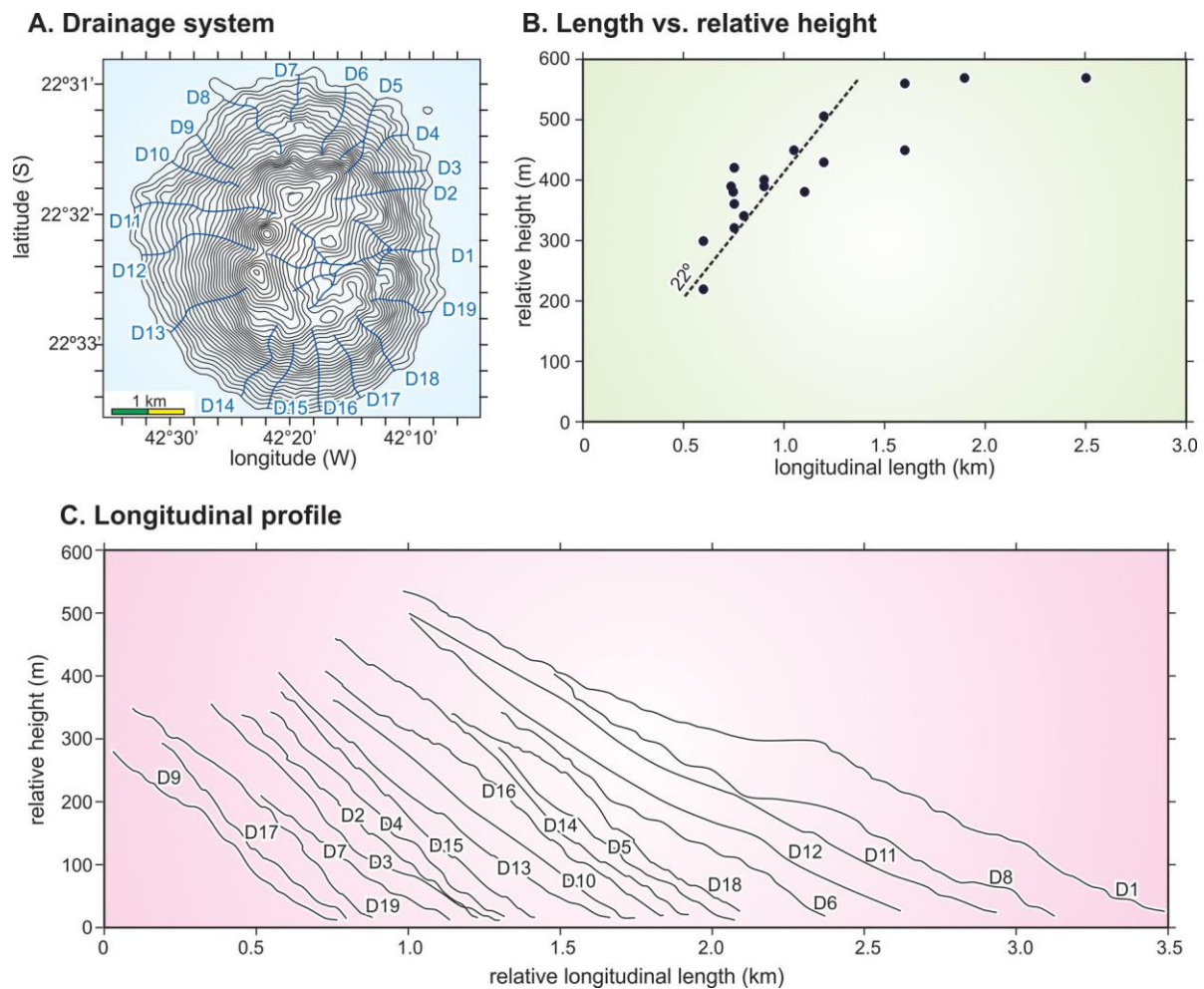


Figure 11. Drainage system of the Morro de São João felsic alkaline intrusive massif, State of Rio de Janeiro, Brazil (A), its declivity (B), and longitudinal profiles (C).

LANDFORM ORIGIN

Morro de São João massif has conical form, so some popular sources, such as newspaper articles and tourism promotion agencies, have diffused an idea of extinct volcano. This urban legend is deeply believed by the local habitants as if a theory proved by scientific studies.

Some of the alkaline intrusive bodies of the Poços de Caldas - Cabo Frio magmatic alignment, such as Itatiaia, Mendanha, Itaúna, Tanguá, Morro dos Gatos, and Cabo Frio Island, have pyroclastic subvolcanic conduits made up mainly of welded tuff breccia (Motoki et al., 2008d). They were emplaced in a depth of 3 km (Motoki & Sichel, 2006; Motoki et al., 2007c) and now exposed on the surface because of the uplift tectonism and the consequent regional denudation (Motoki & Sichel, 2006; Motoki et al., 2007d). The uplift continued up to 40 Ma (Riccomini et al., 2004). That is, the volcanic

eruptions were present but the volcanic edifices are no more preserved.

Geologic researches for the Morro de São João massif (e.g. Brotzu et al., 2007; Mota et al., 2009) clarified that this massif is made up mainly of nepheline syenite, that is, a coarse-grained plutonic rock (Photo 1). The adjacent lowland around this massif exposes orthogneiss of the basement and no rocks of eruptive origin are found. Different from the above-mentioned intrusive bodies, Morro do São João has no volcanic eruption evidence either of the early Cenozoic or of recent times. The geologic studies up to the present confirmed that Morro de São João massif is indubitably not an extinct volcano.

Although it is not a volcano, the silhouette, circular form, and radial drainage system of the Morro de São João have apparent similarities to those of certain volcanoes, such

as Sakurajima volcano, Kyushu Island, Japan (Photo 2).

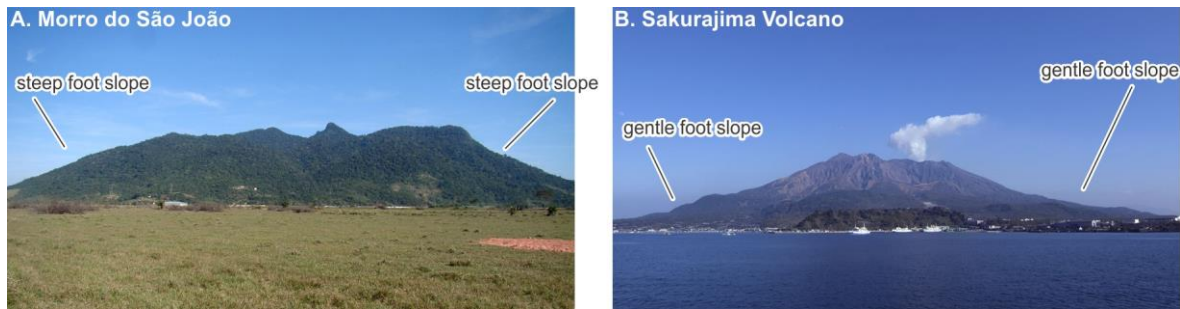


Photo 2. Apparent similarity on the mountain silhouette of the Morro de São João massif (A) and Sakurajima volcano (B). The photo B is credit of Junyoh Tanaka of the GNU free documentation license: <http://pt.wikipedia.org/wiki/Ficheiro:Sakurajima55.jpg>.

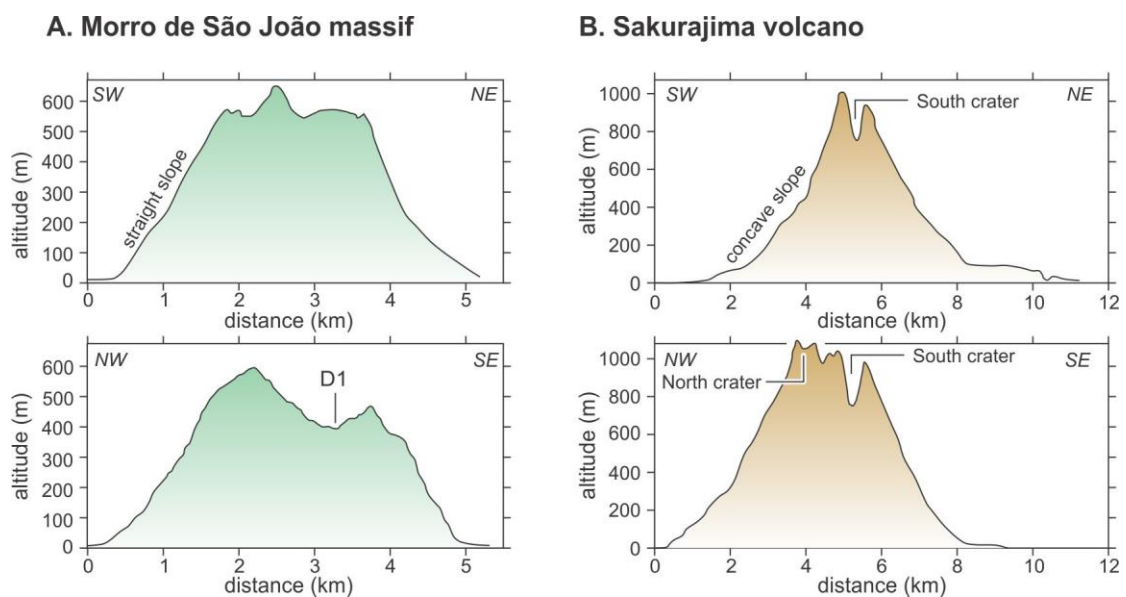


Figure 12. Comparative cross sections base on the ASTER GDEM for: A) Morro de São João massif. State of Rio de Janeiro, Brazil; B) Sakurajima volcano, Kyushu Island, Japan.

In spite of the apparent similarities in the 2D views, there are remarkable morphologic differences in 3D ones: 1) High-angle slope on the foot; 2) Very shallow drainages; 3) Absence of crater; 4) Convex general form.

The marginal scarp of the Morro de São João is steep from the foothill up to the virtual plateau (Photo 2A; Figure 12A). However, young volcanic edifices have gentle on their foot (Photo 2B; Figure 12B). All of the drainages of the Morro de São João, with the exception of D1, are shallow, 20 m deep or less (Figure 11A). The summit level maps interval do not present closed circular morphologic depression on the top of the massif of any grid intervals (Figure 6). The drainage D1 is always

open to the east suggesting that it is originated form conventional erosion and not supposed volcanic crater.

The most highlighted argument is its three-dimensional form of the massif. The MCI for the Morro de São João is -1.2 (Figure 10B), which is lower than that of the felsic alkaline rock bodies of Tanguá (-0.8) and Mendanha (-0.7). That is, the general 3D landform of Morro de São João is the highly convex, being at the opposite side of the volcano landform. The MCI for Sakurajima volcano is (-0.2) being relatively low in the recent volcanic edifices, because of the two craters on the top. The MCI for the Cerro de Diamante Volcano (-0.03) also is relatively low because of a large crater on the top. Even them, the concavity difference

between the young volcanoes and the felsic alkaline intrusive massifs is clear and indubitable, especially for case of the Morro de São João.

The low MCI value of Morro de São João massif can be due to the mechanical firmness and high erosive resistance of the nepheline syenite. Although this rock is

vulnerable to chemical weathering, the effects of weathering passivity protect the massif from erosion (Motoki et al., 2008a).

Consequently, it concluded that the landform of Morro de São João massif is originated from differential erosion of nepheline syenite intrusive body, and not, the supposed extinct volcano.

CONCLUSION

The geomorphological analyses of the Morro de São João felsic alkaline intrusive massif by summit and base level maps with the help of the BAZ system and ASTER GDEM lead to the authors to the following conclusions.

1. The summit level maps show that the Morro de São João massif is characterized by steep marginal scarp of about 30°, virtual plateau of 480 m to 500 m in altitude, and top swell with relative height of about 150 m.
2. The base level maps present, together the summit level maps, expresses that the marginal scarp is steep, indicating high erosive resistance of the constituent nepheline syenite.
3. The maps for the difference between summit and base levels, that is, relief amount maps, demonstrate the existence of high declivity zone along the border of the body and gentle swells area on the central highland.
4. The drainages form a radial system and they are shallow, short, and steep, in average, 20 m deep, 1.1 km long, and of 22° in declivity. Most of the longitudinal profiles are almost straight.
5. The macro concavity index (MCI) for the Morro de São João is -1.2. The Morro de São João massif has highly convex 3D general form and it is widely different from the concave 3D form of young volcanic edifices.
6. The conical morphology of this massif is not attributed to an extinct volcano, but originated from differential erosion of the nepheline syenite intrusive body. This rock has strong erosive resistance because of the mechanical strength and the chemical durability originated from weathering passivity effects.

ACKNOWLEDGEMENT

The present article corresponds to an extended research of the Master Degree thesis of Samuel da Silva, one of the authors, which was concluded in 2010 at the Federal Fluminense University, Niterói, State of Rio de Janeiro, Brazil. The authors are grateful to the FAPERJ, Carlos Chagas Filho Foundation, of the Rio de Janeiro State Government, Brazil, for the financial support of the category APQ1 entitled “Petrologia, geoquímica e magmagêneses dos corpos alcalinos da Ilha de Cabo Frio e Morro de São João e seus aspectos ambientais como patrimônios geológicos”. The authors thank to Dr. Yuji Orihashi of the University of Tokyo for the contact with the ERSDAC.

REFERENCE

1. AIRES, J.R.; MOTOKI, A.; MOTOKI, K.F.; MOTOKI, D.F.; RODRIGUES, J.G. Geomorphological analyses of the Teresópolis Plateau and Serra do Mar Cliff, State of Rio de Janeiro, Brazil with the help of summit level technique and ASTER GDEM, and its relation to the Cenozoic tectonism. *Anuário do Instituto de Geociências da Universidade Federal do Rio de Janeiro*, v. 35, n. 2, p. 105-123, 2012.
2. BROTZU, P.; BECCALUVA, L.; CONTE, A.; FONSECA, M.; GARBARINO, C.; GOMES, C.B., LEONG, R.; MACCIOTTA, G.; MANSUR, R.L.; MELLUSO, L.; MORBIDELLI, L.; RUBERTI, E.; SIGOLO, J.B.; TRAVERSA, G.; VALENÇA, J.G. Petrological and geochemical studies of alkaline rocks from continental Brazil. The syenitic intrusion of Morro Redondo, RJ. *Geochimica Brasiliensis*, v. 3, p. 63-80, 1989.
3. BROTZU, P.; GOMES, C. B.; MELLUSO, L.; MORBIDELLI, L.; MORRA, V.; RUBERTI, E. Petrogenesis of coexisting SiO₂-undersaturated to SiO₂-oversaturated felsic

- igneous rocks: the alkaline complex of Itatiaia, southern eastern Brazil. **Lithos**, v. 40, p. 133-156, 1997.
4. BROTZU, P.; MELLUSO, L.; BENNIO, L.; GOMES, C.B.; LUSTRINO, M.; MORBIDELLI, L.; MORRA, V.; RUBERTI, E.; TASSINARI, C.; D'ANTONIO, M. Petrogenesis of the Early Cenozoic potassic alkaline complex of Morro de São João, southeastern Brazil. **Journal of South American Earth Sciences**, v. 24, p. 93-115, 2007.
 5. CHRYSOULAKIS, N.; ABRAMS, M.; KAMARIANAKIS, Y.; STANISLAWSKI, M. Validation of ASTER GDEM for the Area of Greece. **Photogrammetric engineering and remote sensing**, v. 77, n. 2, p. 157-165, 2011.
 6. DEFFONTAINES, B.; LEE, J.C.; ANGELIER, J.; VARVALHO, J.; RUDANT, J.P. New geomorphic data on the active Taiwan orogen: A multisource approach. **Journal of Geophysical Research**, v.99, n. B10, p. 20243-20666, 1994.
 7. DERBY, O.A. On nepheline-rocks in Brazil - part II. The Tinguá Mass. **The Quarterly Journal of the Geological Society of London**, v. 47, p. 251-265, 1897.
 8. FERHAT, G.; FEIGL, K.L.; RITZ, J.F.; SOURIAU, A. Geodetic measurement of tectonic deformation in the southern Alps and Provence, France, 1947-1994. **Earth and Planetary Science Letters**, v. 159, n. 1-2, p. 35-46, 1998.
 9. GUEDES, E.; HELIBRON, M.; VASCONCELOS, P.M.; VALERIANO, C.M.; ALMEIDA, J.C.H.; TEIXEIRA, W.; THOMÁZ FILHO, A. K-Ar and $^{40}\text{Ar}/^{39}\text{Ar}$ ages of dykes emplaced in the on-shore basement of the Santos Basin, Resende area, SE. Brazil: implications for the south Atlantic opening and Tertiary reactivation. **Journal of South American Earth Sciences**, v. 18, p. 371-182, 2005.
 10. HEILBRON, M. & MACHADO, N. Timing of terrane accretion in the Neoproterozoic-Eopaleozoic Ribeira orogen (se Brazil). **Precambrian Research**, v. 125, p. 87-112, 2003.
 11. HEILBRON, M.; MOHRIAK, W.; VALERIANO, C.M.; MILANI, E.; ALMEIDA, J.C.A., TUPINAMBÁ, M. From collision to extension: the roots of the southeastern continental margin of Brazil. In: Mohriak, W.U. and Talwani, M. (Eds.), **Geophysical Monograph**, American Geophysical Union, v. 115, p. 1-32, 2000.
 12. HIRT, C.; FILMER, M.S.; FEATHERSTONE, W.E. Comparison and validation of the recent freely available ASTER-GDEM ver1, SRTM ver4.1 and GEODATA DEM-9S ver3 digital elevation models over Australia. **Australian Journal of Earth Science**, v. 57, n. 3, p. 337-347, 2010.
 13. HUZITA, K. & KASAMA, T. Kôbe oyobi rinsetsu chiiki chisitu-zu, 1/50,000 (Geologic map of Kobe and the adjacent area, 1/50,000), Edition 3. **Geologic Map**. Secretary of Planning, Municipal district of Kobe, Japan, 1977.
 14. KIRBY, E. & WHIPPLE, K. Quantifying differential rock-uplift rates via stream profile analysis. **Geology**, v. 29-5, p. 415-418, 2001.
 15. KÜHNI, A. & PFIFFNER, O.A. The relief of the Swiss Alps and adjacent areas and its relation to lithology and structure: topographic analysis from a 250-m DEM, **Geomorphology**, v. 41, n. 4, p. 285-307, 2001.
 16. MALENGREAU, B.; LÉNAT, J.F.; FROGER, J.L. Structure of Réunion Island (Indian Ocean) inferred from the interpretation of gravity anomalies. **Journal of Volcanology and Geothermal Research**, v. 88, n. 3, p. 131-146, 1999.
 17. MARTIN, R. Paleogeomorphology and its application to exploration for oil and gas (with examples from Western Canada). **American Association of Petroleum Geology Bulletin**, v. 50, 1966.
 18. MOTA, C.E.M.; GERALDES, M.C.; ALMEIDA, J.C.H.; VARGAS, T.; SOUZA, D.M.; LOUREIRO, R.O.; SILVA, A.P. Características Isotópicas (Nd e Sr), Geoquímicas e Petrográficas da Intrusão Alcalina do Morro de São João: Implicações Geodinâmicas e Sobre a Composição do Manto Sublitosférico. **Revista do Instituto de Geociências - USP, Série Científica**, São Paulo, v. 9, n. 1, p. 85-100, 2009.
 19. MOTOKI, A. & SICHEL, S.E. Avaliação de aspectos texturais e estruturais de corpos vulcânicos e subvulcânicos e sua relação com o ambiente de cristalização, com base em exemplos do Brasil, Argentina e Chile. **REM-Revista Escola de Minas**, Ouro Preto, v. 59, n. 1, p. 13-23, 2006.
 20. MOTOKI, A. & SICHEL, S.E. Hydraulic fracturing as a possible mechanism of dyke-sill transitions and horizontal discordant intrusions in trachytic tabular bodies of Arraial do Cabo, State of Rio de Janeiro, Brazil. **Geofísica Internacional**, Mexico City, v. 47, v. 1, p. 13-25, 2008.
 21. MOTOKI, A.; ZUCCO, L.L.; SICHEL, S.E.; AIRES, J.R.; PETRAKIS, G.H. Desenvolvimento da técnica para especificação digital de cores e a nova nomenclatura para classificação de rochas ornamentais com base nas cores medidas. **Geociências**, Rio Claro, v. 25, n. 4, p. 403-415, 2006.
 22. MOTOKI, A.; SOARES, R.; NETTO, A.M.; SICHEL, S.E.; AIRES, J.R.; LOBATO, M. Geologic occurrence shape of pyroclastic rock dykes in the Dona Eugênia River Valley, Municipal Park of Nova Iguaçu, Rio de Janeiro. **Geociências**, Rio Claro, v. 26, n. 1, p. 67-82, 2007. (a)
 23. MOTOKI, A.; PETRAKIS, G.H.; SOARES, R.S.; SICHEL, S.E.; AIRES, J.R. New method of semi-automatic modal analyses for phenocrysts of porphyritic rocks based on quantitative digital colour specification technique. **Revista Escola de Minas**, Ouro Preto, v. 60, n. 1, p. 13-20, 2007. (b)
 24. MOTOKI, A.; SOARES, R.; NETTO, A.M.; SICHEL, S.E.; AIRES, J.R.; LOBATO, M. Genetic reconsideration of the Nova Iguaçu Volcano model, State of Rio de Janeiro, Brazil: eruptive origin or subvolcanic intrusion? **REM-Revista Escola de Minas**, Ouro Preto, v. 60, n. 4, p. 583-592, 2007. (c)
 25. MOTOKI, A.; SOARES, R.; LOBATO, M.; SICHEL, S.E.; AIRES, J.R. Weathering fabrics in felsic alkaline rocks of Nova Iguaçu, State of Rio de Janeiro, Brazil. **REM-Revista Escola de Minas**, Ouro Preto, v. 60, n. 3, p. 451-458, 2007. (d)
 26. MOTOKI, A.; PETRAKIS, G.H.; SICHEL, S.E.; CARDOSO, C.E.; MELO, R.C.; SOARES, R.S.; MOTOKI, K.F. Landform origin of the Mendanha Massif, State of Rio de Janeiro, Brazil, based on the geomorphological analyses by summit level map technique. **Geociências**, Rio Claro, v. 27, n. 1, p. 99-115, 2008. (a)
 27. MOTOKI, A., SICHEL, S.E., SOARES, R.S., NEVES, J.L.P., AIRES, J.R. Geological, lithological, and petrographical characteristics of the Itaúna Alkaline Intrusive Complex, São Gonçalo, State of Rio de Janeiro, Brazil, with special attention of its emplace mode. **Geociências**, Rio Claro, v. 27, n. 1, p. 33-44, 2008. (b)
 28. MOTOKI, A.; SICHEL, S.E.; SAVI, D.C.; AIRES, J.R. Intrusion mechanism of tabular intrusive bodies of subhorizontal discordant emplacement of the Cabo Frio Island and the neighbour areas, State of Rio de Janeiro, Brazil. **Geociências**, Rio Claro, v. 27, n. 2, p. 207-218, 2008. (c)
 29. MOTOKI, A.; SICHEL, S.E.; SOARES, R.S.; AIRES, J.R.; SAVI, D.C.; PETRAKIS, G.H.; MOTOKI, K.F. Vent-filling pyroclastic rocks of the Mendanha, the Itaúna, and the Cabo Frio Island, State of Rio de Janeiro, Brazil, and their formation process based of the conduit implosion model. **Geociências**, Rio Claro, v. 27, n. 3, p. 451-467, 2008. (d)
 30. MOTOKI, A.; SICHEL, S.E.; CAMPOS, T.F.C.; SRIVASTAVA, N.K.; SOARES, R.S. Present-day uplift rate of the Saint Peter and Saint Paul Islets, Equatorial Atlantic Ocean. **REM-Revista Escola de Minas**, Ouro Preto, v. 62, n. 3, p. 331-342, 2009. (a)
 31. MOTOKI, A.; SICHEL, S.E.; PETRAKIS, G.H. Genesis of the tabular xenoliths along contact plane of the mafic dykes of cabo frio area, state of Rio de Janeiro, Brazil: Thermal delamination or hydraulic shear fracturing? **Geociências**, Rio Claro, v. 28, n. 1, p. 15-26, 2009. (b)
 32. MOTOKI, A.; SICHEL, S.E.; VARGAS, T.; AIRES, J.R.; IWANUCH, W.; MELLO, S.L.M.; MOTOKI, K.F.; SILVA, S.; BALMANT, A.; GONÇALVES, J. Geochemical

- evolution of the felsic alkaline rocks of Tanguá, Rio Bonito, and Itaúna intrusive bodies, State of Rio de Janeiro, Brazil. **Geociências**, Rio Claro, v. 29, n. 3, p. 291-310, 2010.
33. MOTOKI, A.; VARGAS, T.; IWANUCH, W.; SICHEL, S.E.; BALMANT, A.; AIRES, J.R. Tectonic breccia of the Cabo Frio area, State of Rio de Janeiro, Brazil, intruded by Early Cretaceous mafic dyke: Evidence of the Pan-African brittle tectonism? **REM-Revista Escola de Minas**, Ouro Preto, v. 64, n.1, p. 25-36, 2011.
34. MOTOKI, A.; VARGAS, T.; IWANUCH, W.; MELO, D.P.; SICHEL, S.E.; BALMANT, A.; AIRES, J.R.; MOTOKI, K.F. Fossil earthquake evidenced by the silicified tectonic breccia of the Cabo Frio area, State of Rio de Janeiro, Brazil, and its bearings on the genesis of stick-slip fault movement and the associated amagmatic hydrothermalism. **Anuário do Instituto de Geociências da Universidade Federal do Rio de Janeiro**, Rio de Janeiro, v. 35, n. 2, p. 124-139, 2012. (a)
35. MOTOKI, A.; GERALDES, M.C.; IWANUCH, W.; VARGAS, T.; MOTOKI, K.F.; BALMANT, A.; RAMOS, M.N. The pyroclastic dyke and welded crystal tuff of the Morro dos Gatos alkaline intrusive complex, State of Rio de Janeiro, Brazil. **REM-Revista Escola de Minas**, Ouro Preto, v. 65, n. 1, p. 35-45, 2012. (b)
36. MOTOKI, A.; CAMPOS, T.F.C.; FONSECA, V.P.; MOTOKI, K.F. Subvolcanic neck of Cabugi Peak, State of Rio Grande do Norte, Brazil, and origin of its landform. **REM-Revista Escola de Minas**. Ouro Preto, v. 65, n. 2, p. 195-206, 2012. (c)
37. OKUMA, S.; STOTTER, C.; SUPPER, R.; NAKATSUKA, T.; FURUKAWA, R.; MOTSCHKA, K. Aeromagnetic constraints on the subsurface structure of Stromboli Volcano, Aeolian Islands, Italy. **Tectonophysics**, v. 478, n. 1-2, p. 19-33, 2009.
38. PETRAKIS, G.H.; MOTOKI, A.; SICHEL, S.E.; ZUCCO, L.L.; AIRES, J.R.; MELLO S.L.M. Ore geology of special quality gravel and artificial sand: examples of alkaline syenite of Nova Iguaçu, State of Rio de Janeiro, and rhyolite of Nova Prata, State of Rio Grande do Sul, Brazil. **Geociências**, Rio Claro, v. 29, n. 1, p. 21-32, 2009.
39. RÁDOANE, M.; RÁDOANE, N.; DUMITRIU, M. Geomorphological evolution of longitudinal river profiles in the Carpathians. **Geomorphology**, v. 50, p. 293-306, 2003.
40. RICCOMINI, C.; SANT'ANNA, L.G.; FERRARI, A.L. Evolução geológica do rift continental do Sudeste do Brasil. In Mantesso-Neto, V., Bartorelli, A., Carneiro, C.D.R., Brito-Neves, B.B. Ed. **Geologia do Continente Sul-Americano: Evolução da obra de Fernando Flávio Marques de Almeida**. São Paulo. Editora Beca, p. 385-405, 2004.
41. RIIS, F. Quantification of Cenozoic vertical movements of Scandinavia by correlation of morphological surfaces with offshore data. **Global and Planetary Change**, v. 12, n. 1-4, p. 331-357, 1996.
42. RUST, D.; BEHNCKE, B.; NERI, M.; CIOCANEL, A. Nested zones of instability in the Mount Etna volcanic edifice, Italy. **Journal of Volcanology and Geothermal Research**, v. 144, n. 1-4, p. 137-153, 2005.
43. SATO, H. & RAIM. R. Landform analysis using summit level and streamline surface in Abukuma mountains. **Transactions of Japanese Geomorphological Union**, v. 23, n. 3, p. 480-481, 2004.
44. SCHMITT, R.S.; TROUW, R.A.J.; VAN SCHMUS W.R.; PIMENTEL, M.M. Late amalgamation in the central part of West Gondwana: new geochronological data and the characterization of a Cambrian collisional orogeny in the Ribeira Belt (SE Brazil). **Precambrian Research**, v. 133, p. 29-61, 2004.
45. SICHEL, S.E.; MOTOKI, A.; SAVI, D.C.; SOARES, R.S. 2008. Subvolcanic vent-filling welded tuff breccia of the Cabo Frio Island, State of Rio de Janeiro, Brazil. **REM-Revista Escola de Minas**, Ouro Preto, v. 61, n. 4, p. 423-432, 2008.
46. SILVA, S. **Interpretação morfológica baseada nas técnicas de seppômen e sekkokumen dos maciços alcalinos do Estado do Rio de Janeiro**. Niterói, 2010, 123 p. Theiss (Master in Geology) - Instituto de Geociências, Universidade Federal Fluminense. (unpublished)
47. STEWART, S.; TURNER, S.; KELLEY, S.; HAWKESWORTH, C.; KRISTEIN, L.; MANTOVANI, M. 3D - $^{40}\text{Ar}/^{39}\text{Ar}$ geochronology in Paraná continental flood basalt province. **Earth Planet, Science Letters**. v. 143, p. 95-109, 1996.
48. THOMAZ-FILHO, A. & RODRIGUES, A.L. O alinhamento de rochas alcalinas Poços de Caldas-Cabo Frio (RJ) e sua continuidade na Cadeia Vitória-Trindade. **Revista Brasileira de Geociências**, v. 29, n. 2, p. 189-194, 1999.
49. VILARDO, G.; DE NATALE, G.; MILANO, G.; COPPA, U. The seismicity of Mt. Vesuvius. **Tectonophysics**, v. 261, n. 1-3, p. 127-138, 1996.
50. WELLS, S.G.; BULLAR, T.F.; MENGES, C.M.; DRAKE, P.G.; KARA, P.A.; KELSON, K.I.; RITTER, J.B.; WESLING, J.R. Regional variations in tectonic geomorphology along a segmented convergent plate boundary, Pacific coast of Costa Rica. **Geomorphology**. v. 1, p. 239-365, 1988.

*Manuscrito recebido em: 02 de maio de 2011
Revisado e Aceito em: 14 de fevereiro de 2014*